Check for updates

Formation of an MoTe$_2$ based Schottky junction employing ultra-low and high resistive metal contacts†

Sikandar Aftab,[a] Muhammad Waqas Iqbal, [ID] *[b] Amir Muhammad Afzal,[a] M. Farooq Khan,[a] Ghulam Hussain,[b] Hafiza Sumaira Waheed[b] and Muhammad Arshad Kamran [ID] [c]

Schottky-barrier diodes have great importance in power management and mobile communication because of their informal device technology, fast response and small capacitance. In this research, a p-type molybdenum ditelluride (p-MoTe$_2$) based Schottky barrier diode was fabricated using asymmetric metal contacts. The MoTe$_2$ nano-flakes were mechanically exfoliated using adhesive tape and with the help of dry transfer techniques, the flakes were transferred onto silicon/silicon dioxide (Si/SiO$_2$) substrates to form the device. The Schottky-barrier was formed as a result of using ultra-low palladium/gold (Pd/Au) and high resistive chromium/gold (Cr/Au) metal electrodes. The Schottky diode exhibited a clear rectifying behavior with an on/off ratio of $\sim 10^3$ and an ideality factor of ~ 1.4 at zero gate voltage. In order to check the photovoltaic response, a green laser light was illuminated, which resulted in a responsivity of $\sim 3.8 \times 10^3$ A W^{-1}. These values are higher than the previously reported results that were obtained using conventional semiconducting materials. Furthermore, the barrier heights for Pd and Cr with a MoTe$_2$ junction were calculated to be 90 meV and 300 meV, respectively. In addition, the device was used for rectification purposes revealing a stable rectifying behavior.

1. Introduction

Because of their unique semiconductive characteristics, transition metal dichalcogenides (TMDs), have been used for extensive applications in nanoelectronics such as photodetectors,[1–3] and spin-field effect transistors.[4] The TMDs have a band gap of around 1 to 2 eV,[5,6] and demonstrate fascinating electrical and optical properties.[7–10] Molybdenum ditelluride (MoTe$_2$) can be reduced to a monolayer or a few layers from its bulk form using adhesive tape through mechanical exfoliation.[10] As found from previous reports, MoTe$_2$ in its bulk form shows an indirect band gap of 0.88 eV, whereas its monolayer has a direct band-gap of 1.02 eV.[8,11,12] The mobility for few-layered MoTe$_2$ lies in the range of 0.2–40 cm^2 V^{-1} s^{-1}.[13–16] Furthermore, use of MoTe$_2$ has been shown to be favorable for many applications in environmental sensing, light emitting diodes and photosensors.[17,18]

The two-dimensional (2D) material-based junctions have shown outstanding properties such as optical absorption, charge transportation and band alignment for optoelectronic and electronic applications.[19,20] Until now, the study has mainly been based on heterojunctions comprising p–n junctions for practical uses of 2D materials, however semiconductor/metal Schottky barrier diodes (SBD) have not been studied extensively.[21,22] The SBD is formed by a contact effect of metal and a semiconductive material which is the simplest structure amongst modern electronic devices.[23] The SBDs have been shown to be promising for applications in electronic devices, for example, as photodiodes, power diodes, sensors, and integrated circuits.[24,25] Schottky-barrier diodes have great importance in power management and mobile communications because of their informal device technology, fast response and small capacitance.[26,27] In particular, Schottky diodes are majority carrier devices and because they are single carrier devices, they have advantages because of the junction diode which is a bipolar-device.

The interface properties of metal and semiconductor are influenced by the conductivity type of the charge carrier. The metal and semiconductor interface be either a rectifying type or an ohmic type, and is roughly dependent on the work function values of them. For example, a semiconductor material with n-type conductivity would show rectifying behavior with metals having greater work function values and show ohmic behavior

[a]Department of Physics and the Astronomy and Graphene Research Institute, Sejong University, Seoul 05006, Korea

[b]Department of Physics, Riphah Institute of Computing and Applied Sciences (RICAS), Riphah International University, 14 Ali Road, Lahore, Pakistan. E-mail: waqas.iqbal@riphah.edu.pk

[c]Department of Physics, College of Science, Majmaah University, PO Box No. 1712, Al-Zulfi 11932, Saudi Arabia

† Electronic supplementary information (ESI) available. See DOI: 10.1039/c8ra09656b

with those having low work function values. However, semiconductors with p-type conductivity exhibit the opposite characteristics. The Schottky barrier because of a difference of Fermi level of the semiconductor and the work function of the metal, play an important role to determine the performance of a diode.[28–30]

In this research, the MoTe$_2$ based field effect transistor (FET) is formed by using asymmetric metals contacts chromium/gold (Cr/Au) and palladium/gold (Pd/Au) to understand the charge carrier transport and the interface characteristics at the junction. It is found that MoTe$_2$ forms an ohmic contact with Pd/Au whereas a Schottky barrier is observed with Cr/Au. In addition, an excellent photo response and gate-dependent behavior was found for the Schottky diode. A rectification ratio of up to 10^3

was calculated for the device. Furthermore, traditional thermionic emission theory was applied to determine the values of the Schottky barrier heights for individual metal contacts. The results obtained suggested that there would be useful technological applications for the Schottky diodes based on MoTe$_2$.

2. Experimental

Natural bulk crystals of p-type molybdenum ditelluride (p-MoTe$_2$) were exfoliated with adhesive tape and a dry transfer technique was used to transfer the flakes onto silicon/silicon dioxide (Si/SiO$_2$) substrates with the help of a transparent poly(dimethylsiloxane) (PDMS) stamp. Multilayered p-MoTe$_2$ nanoflakes were identified using Raman spectroscopy, optical
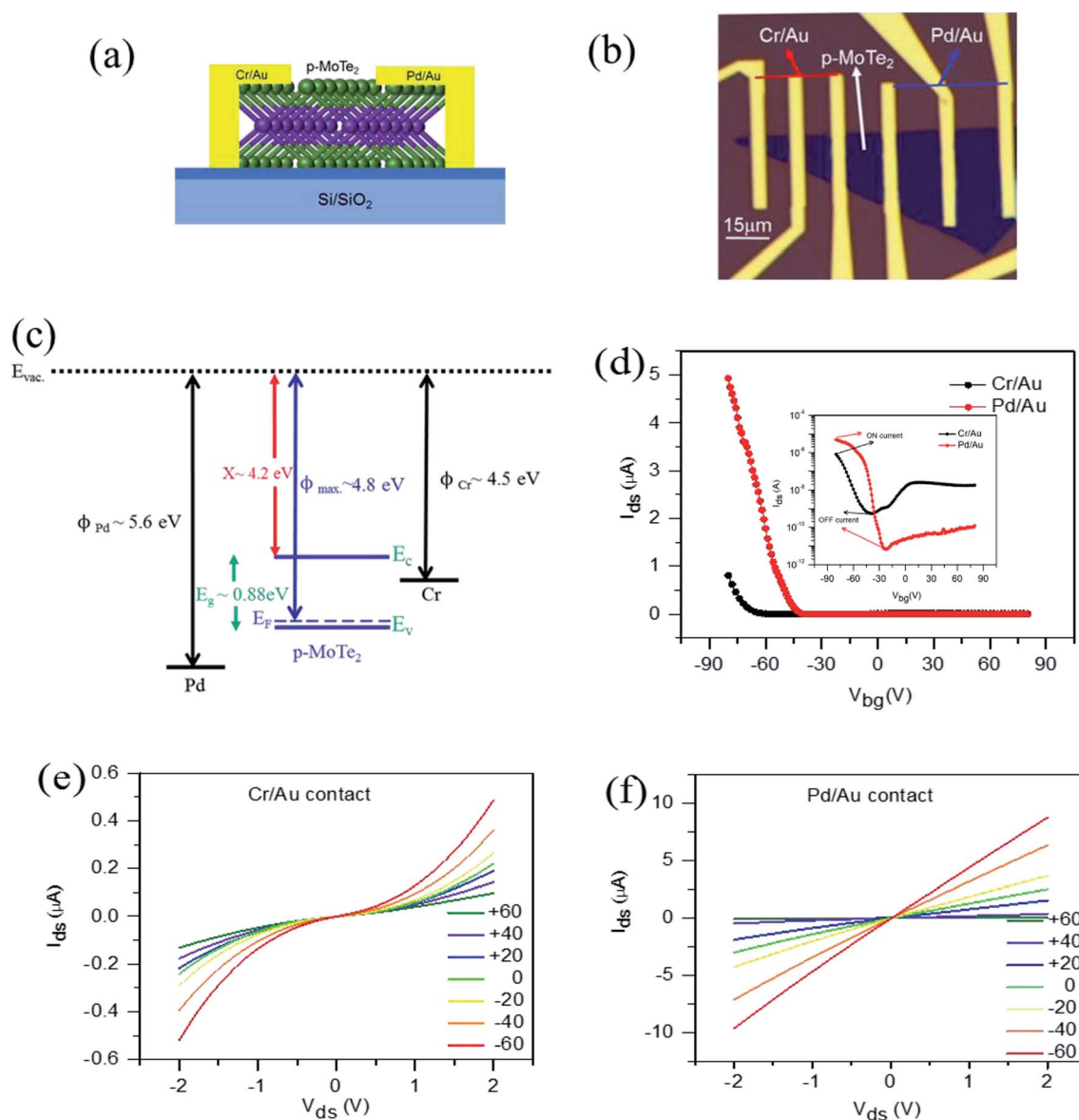

Fig. 1 (a) Schematic illustration of the MoTe$_2$ Schottky diode. (b) Optical microscope image of the device. (c) Band profile of Pd/MoTe$_2$/Cr. (d) Transfer characteristics of p-MoTe$_2$ with Pd/Au and Cr/Au FETs with $V_{ds} = 0.5$ V. The I_D–V_D characteristics as a function of gate bias, (e) ultra-high resistive metal contact effect of p-MoTe$_2$ with Cr/Au, and (f) ultra-low resistive ohmic metal contact behavior of MoTe$_2$ with Pd/Au.

microscopy and the results obtained were also confirmed using atomic force microscopy (AFM). Electrodes were made using e-beam lithography by depositing Pd/Au (8/10 nm) and Cr/Au (8/10 nm), onto the p-MoTe$_2$ FET. The electrical transport measurements both at room and low temperatures were performed using the semiconductor characterization systems, Keithley 2400 Source Meter and Keithley 6485 Picoammeter.

3.   Results and discussion

The device is illustrated schematically in Fig. 1a and the optical image of the device is shown in Fig. 1b. The p-MoTe$_2$ nanoflakes were exfoliated from their bulk form and using a dry transfer technique with a PDMS stamp were transferred onto the Si/SiO$_2$ substrate. Fig. S1(a) (ESI†) shows the typical AFM image of p-MoTe$_2$ FET on the SiO$_2$ substrate. In addition the height profile for p-MoTe$_2$ flakes with a thickness of ∼8 nm from the AFM image was obtained, and the results are shown in Fig. S1(b) (ESI†). Fig. S3 (ESI†) shows the Raman spectra of few-layer p-MoTe$_2$ obtained using an excitation laser with a wavelength of 514 nm. Three peaks of MoTe$_2$ were observed: A$_{1g}$ mode at ∼173.5 cm^{-1}, E$_{2g}^1$ mode at ∼235.2 cm^{-1}, and B$_{2g}^1$ mode at ∼290.8 cm^{-1}.[1]

Metals having larger values of work function are favorable for p-MoTe$_2$ to form a shallow Schottky barrier whereas with low values of work function they show a greater barrier height.[29,30] It was found that MoTe$_2$ and the metal interface could be either an ohmic type or rectifying in nature depending on the work function of both the metals and the semiconductor. Pd ($\phi = 5.6$ eV)[31] and Cr ($\phi = 4.5$ eV)[32] were selected as the high and low work function metals, respectively, as shown in Fig. 1c.

Initially, the electrical performance of the device with source/drain Cr/Au and Pd/Au contacts was measured. For both configurations, p-MoTe$_2$ showed strong p-type conduction as shown in Fig. 1d. The field-effect carrier mobility (μ_{FE}) was calculated for individual metal contacts using the following equation:

$$\mu_{FE} = \frac{L}{W}\left(\frac{dI_{ds}}{dV_{bg}}\right)\frac{1}{C_{bg}V_{ds}}$$

where W and L are the channel width and length, respectively, C_{bg} is the gate capacitance (∼115 aF μm^{-2}) for the Si/SiO$_2$ substrate and $\left(\frac{dI_{ds}}{dV_{bg}}\right)$ is the slope of the transfer characteristics. The hole mobility for the Cr/Au contacts was found to be 1.2 cm^2 V^{-1} s^{-1} with a current on/off ratio of 10^3 whereas the hole mobility for the Pd/Au electrodes was found to be 7.0 cm^2 V^{-1} s^{-1} with an on/off ratio of around 10^6 at $V_{ds} = 0.5$ V. These findings revealed improved electrical characteristics when Pd/Au were contacted with MoTe$_2$ rather than Cr/Au, which could be because of the formation of an ohmic contact and also be because of the use of a high work function metal (Pd with a work function $\phi = 5.6$ eV).[31] Also, in Fig. 1c it is clearly indicated in the band profile that the Fermi level of Pd is deeper than the Fermi level of MoTe$_2$.

In addition, the I_D–V_D output characteristics were measured as a function of the back gate voltage (V_{bg}) which illustrated

rectifying behavior for the Cr/Au metal contacts because of the formation of the Schottky barrier with p-MoTe$_2$ (Fig. 1e), whereas ohmic contact is formed with Pd/Au because of linear I–V characteristics as shown in Fig. 1f.

The output characteristics using Pd/Au and Cr/Au asymmetric electrodes showed a clear gate-dependent rectification behavior, particularly at negative gate bias voltages because of the high Schottky barrier height between Cr and MoTe$_2$ as shown in Fig. 2a. The forward current increased steadily as a result of thinning the barrier. The rectification ratio could be defined as the ratio of reverse current (I_r) to forward current (I_f) at same $\pm V_{ds}$.[33] The rectification ratio changed from 5.2 × 10^1 to 1.9 × 10^3 with variation in gate bias as shown in Fig. 2b. The Schottky diode showed a better rectification ratio at a negative gate bias because of the reduction of the reverse leakage current because of greater band banding of the semiconductor with respect to the metal's Fermi level.[21,22]

Furthermore, the rectifying performance of the Schottky diode was studied by determining the ideality factor using the Shockley diode equation:[34,35]
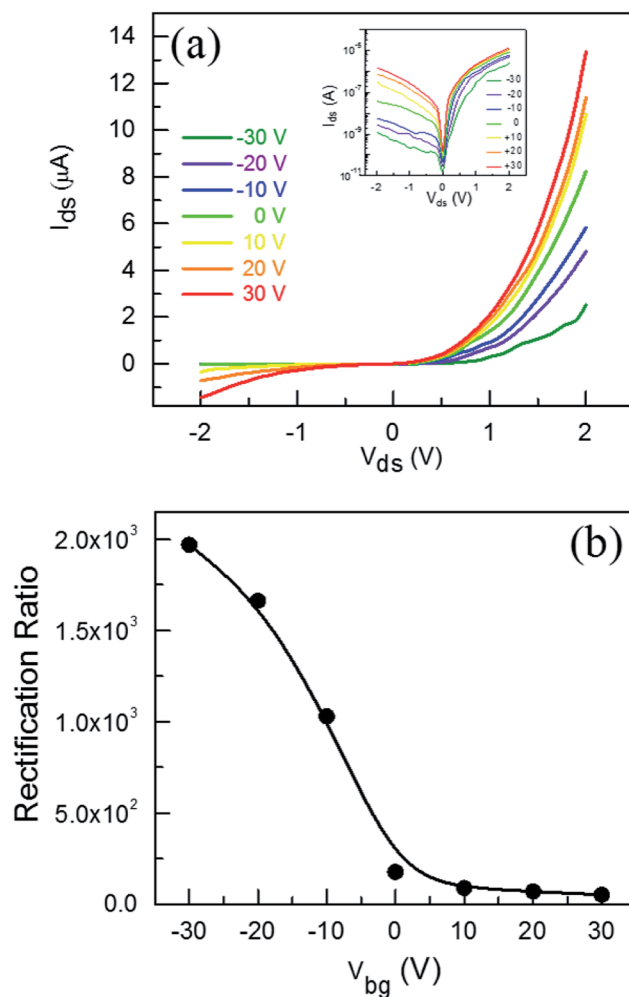

Fig. 2 (a) Gate-dependent rectifying effect of MoTe$_2$ Schottky junction between Cr/Au–Pd/Au contacts. (b) Rectification ratio as a function of the back gate of MoTe$_2$ Schottky junction.

$$I_D = I_S \left[\exp\left(\frac{qV}{nK_B T} \right) - 1 \right]$$

where I_D and I_S are the diode and reverse bias saturation currents, respectively, V is the applied voltage across the diode, n is an ideality factor, q is an electronic charge, T is the temperature and K_B is the Boltzmann constant. For voltage > $K_B T$ (e.g., > 0.1 V), the previous equation becomes:

$$\ln(I_D) = \ln(I_S) + \left(\frac{q}{nK_B T} \right) V$$

The slope from the plot of the natural logarithm of the diode current *versus* the applied voltage gives $q/nK_B T$, which gives n. The lowermost value of n is found to be ∼1.4. The temperature dependent transfer characteristics were also measured, as shown in Fig. S2 (ESI†), to extract the Schottky barrier height (SBH) of Pd ($\phi = 5.6$ eV)[31] and Cr ($\phi = 4.5$ eV).[32] In this research, metal contacts were exclusively made of Pd and Cr and were directly adhered to the 2D semiconductor (MoTe$_2$).

According to traditional thermionic emission theory, the following equation was used:[36–38]

$$I_{ds} = A_{device} A^* T^2 \exp\left[-\frac{q}{K_B T} \left(\Phi_B - \frac{V_{ds}}{n} \right) \right]$$

where A_{device} and A^* are the area of the detector and Richardson constant, respectively, q is the elementary charge of the electron, T is the temperature, K_B is the Boltzmann constant, V_{ds} the source-drain voltage, and n is the ideality factor. Fig. 3a and c show the Arrhenius plot of the device at various gate overdrive voltages for Cr and Pd, respectively. By taking the slope of $\ln(I_{ds}/T^2)$ *versus* $1000/T$, the SBH for Pd and MoTe$_2$ was calculated to be about ∼90 meV, whereas the extracted SBH for Cr and MoTe$_2$ was about ∼300 meV as shown in Fig. 3b and c, respectively. The value of Φ_B (SBH), taking into consideration the Schottky–Mott rule, is the variation in metal work function (Φ_{metal}) and semiconductor electron affinity (χ_{semi}):

$$\Phi_B = \Phi_{metal} - \chi_{semi}.$$

However, a number of semiconductors differ from the previously mentioned rule ever since the establishment of metal-induced gap states,[39,40] which are occupied with electrons and shift the middle of the bandgap nearer to the Fermi level and this effect is known as Fermi level pinning.[31,41] For example, p-MoTe$_2$ had a stronger Fermi level pinning with Pd metal.[31]
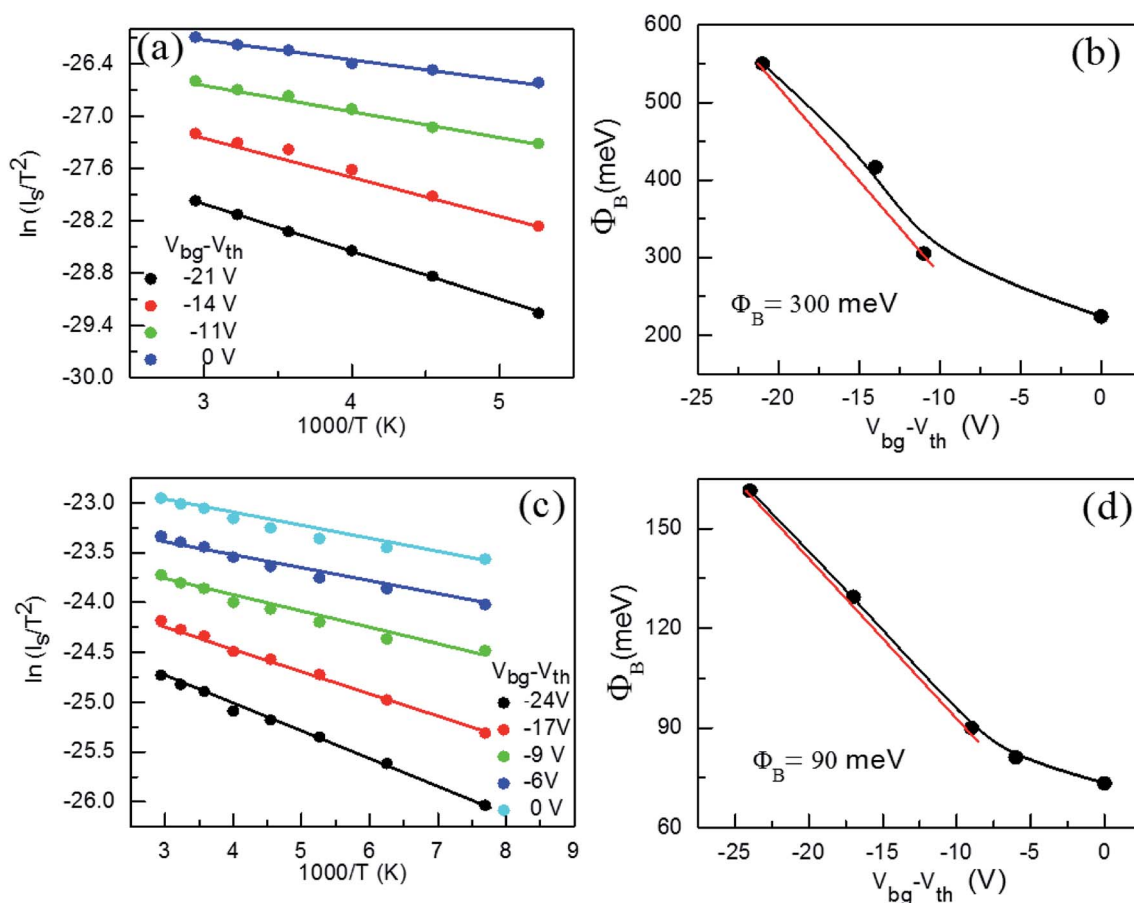

Fig. 3 (a) Conventional Richardson plot ln(I/T^2) *versus* $1000/T$ for Cr/Au metal contacts. (b) The potential barrier height at the MoTe$_2$/Cr/Au junction as a function of $V_{bg}-V_{th}$. (c) Conventional Richardson plot ln(I/T^2) *versus* $1000/T$ for Pd/Au metal contacts. (d) The potential barrier height at the MoTe$_2$/Pd/Au junction as a function of $V_{bg}-V_{th}$.

However, the barrier height between Cr and $MoTe_2$ was higher than that between Pd and $MoTe_2$, which was the reason for the ohmic behavior of the $MoTe_2$ and Pd/Au junction. Under forward biasing, if the Cr metal is connected with a negative bias, forward biasing would result in the holes being attracted to the interface as a result of a decrease in barrier height. Instead, under reverse biasing, if the Cr metal is connected with a positive terminal, reverse biasing would result in the holes being removed from the interface of the metal and semiconductor as a result of increased barrier height. So in the forwarding biased region the net current is larger, while in the reverse biasing region it is very low.

In addition, the photoresponse characteristics of the $MoTe_2$ Schottky diode were also demonstrated. Under forwarding biasing the linear output characteristics were measured using asymmetric metal contacts, under light illumination with a green laser light with a wavelength of about 530 nm having a power of 1.2 mW cm^{-2} as shown in Fig. 4. At the forward biased region, the dark current was very low because of the ultra-high resistive metal contact between Cr and $MoTe_2$. Upon illumination with green laser light, the photo-responsivity (R) of the Schottky junction was calculated using the equation:

$$R = \frac{I_{ph}}{P_{Laser \times A}}$$

where I_{ph} is the photocurrent and P_{Laser} is the laser power.[42,43] The calculated responsivity was 3.8×10^3 A W^{-1} which was higher than that previously reported for Schottky junctions based on conventional semiconductor materials.[23,44]

In addition, the Schottky diode was tested for the application of rectification, and which rectified output voltage signals by applying both AC square and sine waves. Fig. 5 presents the dynamic rectified V_{In}–V_{Out} curves of the device at an external resistance of 1 MΩ by applying the AC sine and square input voltage signal sweeping from −5 to +5 V at 10 Hz.
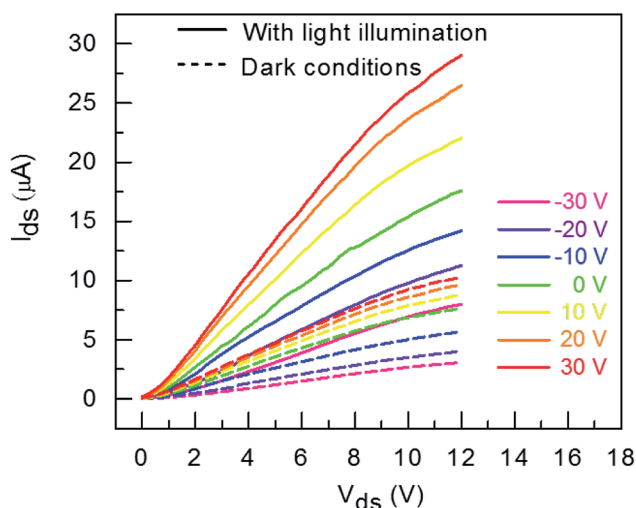

Fig. 4 Output characteristics of the Schottky diode (Cr/Au–Pd/Au) with the positive bias as a function of gate bias.
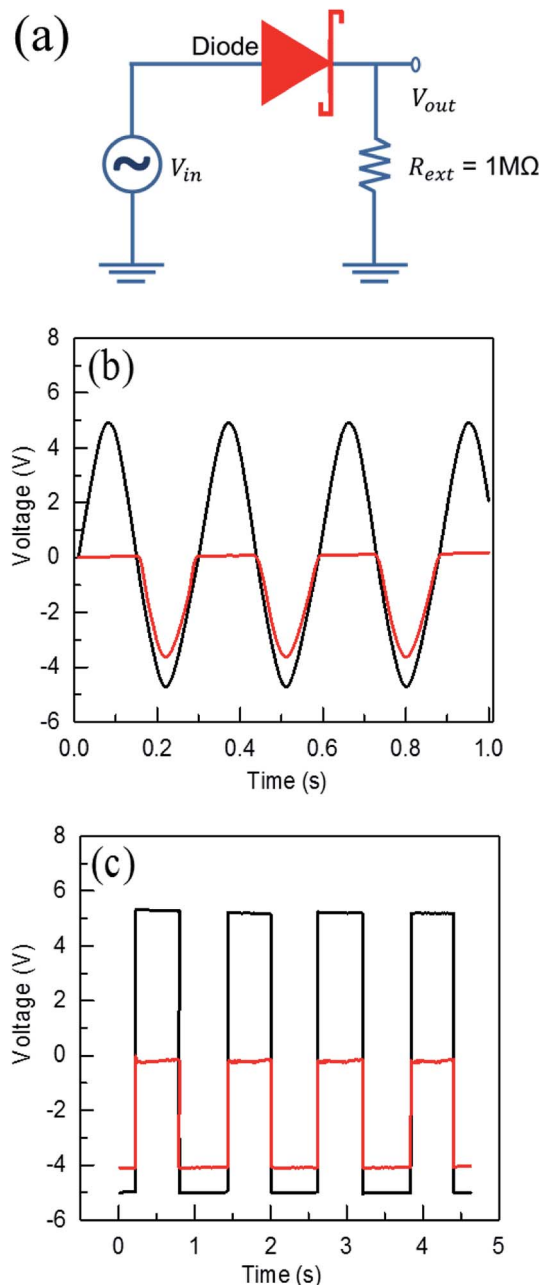

Fig. 5 (a) Schematic illustration to demonstrate the dynamic rectification of a Schottky diode. Demonstration of rectified dynamic output of the Schottky diode by applying (b) AC sine and (c) square wave signals with a series resistor of resistance 1 MΩ. V_{In} = ±5 V at 10 Hz.

4. Conclusions

In summary, a Schottky barrier diode was formed, based on a p-$MoTe_2$ FET, which demonstrated excellent photo response and gate-dependent behavior. The Schottky diode showed a clear rectifying behavior with an on/off ratio reaching up to 10^3 and with an ideality factor of ~1.4 at zero gate voltage. In order to check the photovoltaic response, the diode was illuminated with green laser light, and the responsivity was 3.8×10^3 A W^{-1}, which was higher than the previously reported values based on

conventional semiconductor materials. The barrier heights for Pd and Cr with a $MoTe_2$ junction were calculated to be 90 meV and 300 meV, respectively. In addition, the device was used for rectification and revealed stable rectifying behavior. The outcomes of this research can be applied in future electronics which require high speed and low noise performance.

Conflicts of interest

There are no conflicts to declare.

Acknowledgements

References

1 O. Lopez-Sanchez, D. Lembke, M. Kayci, A. Radenovic and A. Kis, *Nat. Nanotechnol.*, 2013, **8**, 497–501.

2 C. Lan, C. Li, Y. Yin and Y. Liu, *Nanoscale*, 2015, **7**, 5974–5980.

3 N. Perea-López, A. L. Elías, A. Berkdemir, A. Castro-Beltran, H. R. Gutiérrez, S. Feng, R. Lv, T. Hayashi, F. López-Urías and S. Ghosh, *Adv. Funct. Mater.*, 2013, **23**, 5511–5517.

4 J. Klinovaja and D. Loss, *Phys. Rev. B: Condens. Matter Mater. Phys.*, 2013, **88**, 075404.

5 B. Radisavljevic, A. Radenovic, J. Brivio, I. V. Giacometti and A. Kis, *Nat. Nanotechnol.*, 2011, **6**, 147–150.

6 T. Georgiou, R. Jalil, B. D. Belle, L. Britnell, R. V. Gorbachev, S. V. Morozov, Y.-J. Kim, A. Gholinia, S. J. Haigh and O. Makarovsky, *Nat. Nanotechnol.*, 2013, **8**, 100–103.

7 S. Fathipour, N. Ma, W. Hwang, V. Protasenko, S. Vishwanath, H. Xing, H. Xu, D. Jena, J. Appenzeller and A. Seabaugh, *Appl. Phys. Lett.*, 2014, **105**, 192101.

8 C. Ruppert, O. B. Aslan and T. F. Heinz, *Nano Lett.*, 2014, **14**, 6231–6236.

9 M. Yamamoto, S. T. Wang, M. Ni, Y.-F. Lin, S.-L. Li, S. Aikawa, W.-B. Jian, K. Ueno, K. Wakabayashi and K. Tsukagoshi, *ACS Nano*, 2014, **8**, 3895–3903.

10 B. Chamlagain, Q. Li, N. J. Ghimire, H.-J. Chuang, M. M. Perera, H. Tu, Y. Xu, M. Pan, D. Xaio and J. Yan, *ACS Nano*, 2014, **8**, 5079–5088.

11 I. G. Lezama, A. Arora, A. Ubaldini, C. Barreteau, E. Giannini, M. Potemski and A. F. Morpurgo, *Nano Lett.*, 2015, **15**, 2336–2342.

12 I. G. Lezama, A. Ubaldini, M. Longobardi, E. Giannini, C. Renner, A. B. Kuzmenko and A. F. Morpurgo, *2D Mater.*, 2014, **1**, 021002.

13 C. Pan, Y. Fu, J. Wang, J. Zeng, G. Su, M. Long, E. Liu, C. Wang, A. Gao and M. Wang, *Adv. Electron. Mater.*, 2018, **4**, 1700662.

14 Y. F. Lin, Y. Xu, S. T. Wang, S. L. Li, M. Yamamoto, A. Aparecido-Ferreira, W. Li, H. Sun, S. Nakaharai and W. B. Jian, *Adv. Mater.*, 2014, **26**, 3263–3269.

15 D. H. Keum, S. Cho, J. H. Kim, D.-H. Choe, H.-J. Sung, M. Kan, H. Kang, J.-Y. Hwang, S. W. Kim and H. Yang, *Nat. Phys.*, 2015, **11**, 482.

16 S. Nakaharai, M. Yamamoto, K. Ueno, Y.-F. Lin, S.-L. Li and K. Tsukagoshi, *ACS Nano*, 2015, **9**, 5976–5983.

17 Y. F. Lin, Y. Xu, C. Y. Lin, Y. W. Suen, M. Yamamoto, S. Nakaharai, K. Ueno and K. Tsukagoshi, *Adv. Mater.*, 2015, **27**, 6612–6619.

18 Y.-Q. Bie, G. Grosso, M. Heuck, M. M. Furchi, Y. Cao, J. Zheng, D. Bunandar, E. Navarro-Moratalla, L. Zhou and D. K. Efetov, *Nat. Nanotechnol.*, 2017, **12**, 1124.

19 Y. Deng, Z. Luo, N. J. Conrad, H. Liu, Y. Gong, S. Najmaei, P. M. Ajayan, J. Lou, X. Xu and P. D. Ye, *ACS Nano*, 2014, **8**, 8292–8299.

20 W. Hu and J. Yang, *J. Mater. Chem. C*, 2017, **5**, 12289–12297.

21 A. Di Bartolomeo, A. Grillo, F. Urban, L. Iemmo, F. Giubileo, G. Luongo, G. Amato, L. Croin, L. Sun and S. J. Liang, *Adv. Funct. Mater.*, 2018, **28**, 1800657.

22 A. Di Bartolomeo, F. Urban, M. Passacantando, N. McEvoy, L. Peters, L. Iemmo, G. Luongo, F. Romeo and F. Giubileo, *Nanoscale*, 2019, **11**, 1538–1548.

23 T.-Y. Oh, S. Woo Jeong, S. Chang, K. Choi, H. Jun Ha and B. Kwon Ju, *Appl. Phys. Lett.*, 2013, **102**, 021106.

24 Y. Zhao, X. Xiao, Y. Huo, Y. Wang, T. Zhang, K. Jiang, J. Wang, S. Fan and Q. Li, *ACS Appl. Mater. Interfaces*, 2017, **9**, 18945–18955.

25 J. Miao, S. Zhang, L. Cai and C. Wang, *Adv. Electron. Mater.*, 2016, **2**, 1500346.

26 J. B. Soole and H. Schumacher, *IEEE J. Quantum Electron.*, 1991, **27**, 737–752.

27 S. Averin, R. Sachot, J. Hugi, M. De Fays and M. Ilegems, *J. Appl. Phys.*, 1996, **80**, 1553–1558.

28 M. Yang, K. Teo, W. Milne and D. Hasko, *Appl. Phys. Lett.*, 2005, **87**, 253116.

29 M. Hughes, K. Homewood, R. Curry, Y. Ohno and T. Mizutani, *Appl. Phys. Lett.*, 2013, **103**, 133508.

30 B. Ryu, Y. T. Lee, K. H. Lee, R. Ha, J. H. Park, H.-J. Choi and S. Im, *Nano Lett.*, 2011, **11**, 4246–4250.

31 C. Kim, I. Moon, D. Lee, M. S. Choi, F. Ahmed, S. Nam, Y. Cho, H.-J. Shin, S. Park and W. J. Yoo, *ACS Nano*, 2017, **11**, 1588–1596.

32 N. Dhar, T. Chowdhury, M. Islam, N. Khan, M. Rashid, M. Alam, Z. Alothman, K. Sopian and N. Amin, *Chalcogenide Lett.*, 2014, **11**, 271–279.

33 F. Liu, W. L. Chow, X. He, P. Hu, S. Zheng, X. Wang, J. Zhou, Q. Fu, W. Fu and P. Yu, *Adv. Funct. Mater.*, 2015, **25**, 5865–5871.

34 D. A. Neamen, *Semiconductor physics and devices*, McGraw-Hill, New York, 1997.

35 T. Banwell and A. Jayakumar, *Electron. Lett.*, 2000, **36**, 291–292.

36 J. H. Lee, H. Z. Gul, H. Kim, B. H. Moon, S. Adhikari, J. H. Kim, H. Choi, Y. H. Lee and S. C. Lim, *Nano Lett.*, 2017, **17**, 673–678.

37 A. Allain, J. Kang, K. Banerjee and A. Kis, *Nat. Mater.*, 2015, **14**, 1195.

38 S. Das, H.-Y. Chen, A. V. Penumatcha and J. Appenzeller, *Nano Lett.*, 2012, **13**, 100–105.

39 K.-A. Min, J. Park, R. M. Wallace, K. Cho and S. Hong, *2D Materials*, 2016, **4**, 015019.

40 S. Picozzi, A. Continenza, G. Satta, S. Massidda and A. Freeman, *Phys. Rev. B: Condens. Matter Mater. Phys.*, 2000, **61**, 16736.

41 P. Bampoulis, R. Van Bremen, Q. Yao, B. Poelsema, H. J. Zandvliet and K. Sotthewes, *ACS Appl. Mater. Interfaces*, 2017, (46), 39860–39871.

42 M. M. Furchi, A. Pospischil, F. Libisch, J. Burgdörfer and T. Mueller, *Nano Lett.*, 2014, **14**, 4785–4791.

43 L. Ye, H. Li, Z. Chen and J. Xu, *ACS Photonics*, 2016, **3**, 692–699.

44 A. Rochas, A. R. Pauchard, P.-A. Besse, D. Pantic, Z. Prijic and R. S. Popovic, *IEEE Trans. Electron Devices*, 2002, **49**, 387–394.